

## The Panarea CO<sub>2</sub> vent: A natural laboratory for investigating the effect of ocean acidification on marine biodiversity

Finanziato dall'Unione Europea - NextGenerationEU a valere sul Piano Nazionale di Ripresa e Resilienza (PNRR) – Missione 4 Istruzione e ricerca – Componente 2 Dalla ricerca all'impresa - Investimento Investimento 1.4 , Avviso D. D. 3138 del 12/16/2021 rettificato con D.D. 3175 del 18/12/2021, dal titolo: National Biodiversity Future Center, codice proposta CN00000033 - CUP J33C22001190001

### The experimental site

The Island of Panarea belongs to the Aeolian Archipelago (Italy), located in the southern Tyrrhenian Sea in the Mediterranean (Figure 1), and is part of an active volcanic system (De Astis et al. 2003).

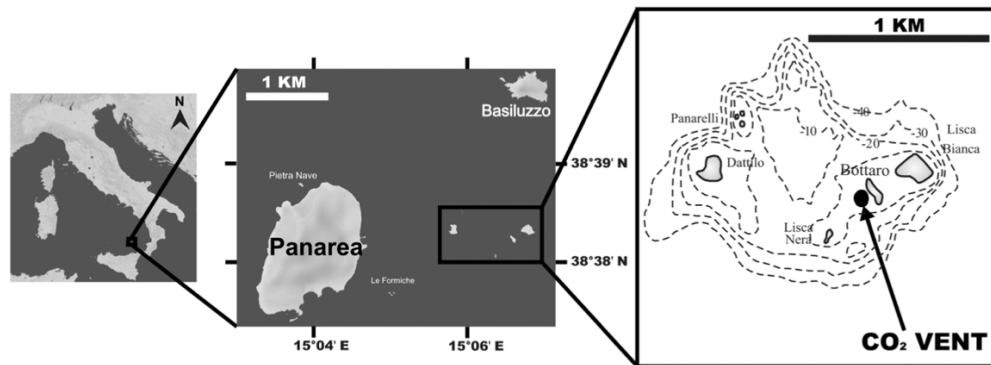


Figure 1. Map of the study site off Panarea Island (Aeolian Archipelago, Italy). Insets show the location of the vent area, SE of Bottaro.

The main vent is a crater 20 x 14 m wide and 10 m deep that generates a sustained column of bubbles (Figure 2) (98–99% CO<sub>2</sub>) at ambient temperature, without toxic compounds such as metals and H<sub>2</sub>S, thus generating a natural pH gradient extending for ~ 34 m (see video: [https://static-content.springer.com/esm/art%3A10.1038%2Fncclimate2241/MediaObjects/41558\\_2014\\_BFncclimate2241\\_MOESM396\\_ESM.wmv](https://static-content.springer.com/esm/art%3A10.1038%2Fncclimate2241/MediaObjects/41558_2014_BFncclimate2241_MOESM396_ESM.wmv) from Goffredo et al. 2014; Figures 2 and 3). Seawater physical-chemical parameters have been extensively characterized in three Sites along this gradient (Goffredo et al. 2014, Fantazzini et al. 2015, Prada et al. 2017), namely: Site 1 (pH total scale [pH<sub>Ts</sub>] = 8.1; 95% confidence intervals [CI] = 8.0–8.1), which is considered as a control, Site 2 (pH<sub>Ts</sub> = 7.9; 95% CI = 7.8–7.9) which aligns with IPCC's mean pH prediction of a conservative CO<sub>2</sub> emissions scenario (Representative Concentration Pathway, RCP6.0), and Site 3 (pH<sub>Ts</sub> = 7.7; 95% CI = 7.7–7.8) which fits the “business-as-usual” CO<sub>2</sub> emissions scenario for the end of the century (RCP8.5). The pH changes are accompanied by significant shifts in carbonate-bicarbonate equilibria, with average aragonite saturation decreasing by more than 40% from Site 1 to Site 3 (Table 1; Figure 3).

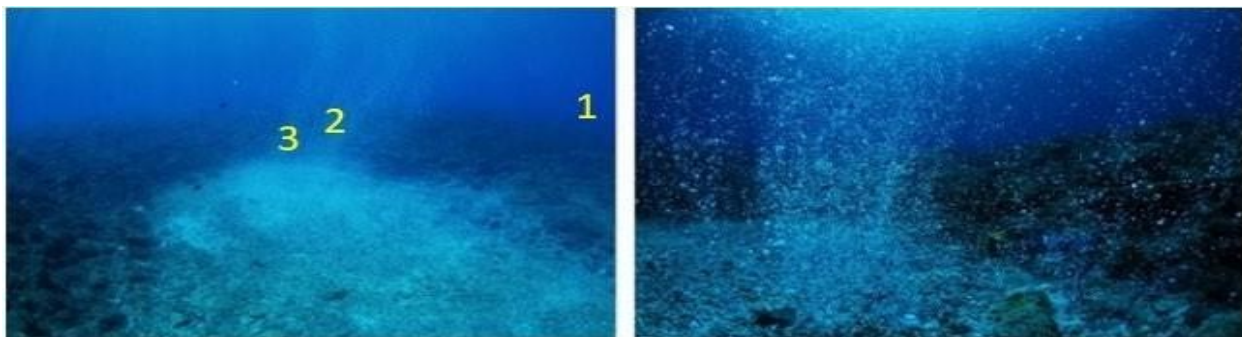


Figure 2. Representative pictures of the Panarea crater (left; numbers indicate study Sites 1-3) and CO<sub>2</sub> bubbling from the seafloor (right).

Table 1. Seawater carbonate chemistry. Measurements are shown for each study Site off the Island of Panarea. Site 1 is the reference and sites 2 and 3 are the elevated  $p\text{CO}_2$  Sites.

Measured Parameters					
Treatment	pH range (total scale)	T (°C)	TA ( $\mu\text{mol kg}^{-1}$ )	S (%)	
Site 1	8.07 (7.82-8.45)	20.5 (14.3-26.0)	2438 (2368-2600)	37 (33-38)	
Site 2	7.87 (7.54-8.25)	20.7 (14.4-26.0)	2429 (2334-2618)	37 (33-38)	
Site 3	7.74 (7.05-8.21)	20.6 (14.4-26.0)	2426 (2343-2610)	37 (34-38)	
Statistical significance	***	NS	NS	NS	
Calculated Parameters					
Treatment	* $p\text{CO}_2$ ( $\mu\text{atm}$ )	* $\text{HCO}_3^-$ ( $\mu\text{mol kg}^{-1}$ )	* $\text{CO}_3^{2-}$ ( $\mu\text{mol kg}^{-1}$ )	*DIC ( $\mu\text{mol kg}^{-1}$ )	* $\Omega_{\text{arag}}$
Site 1	391 (127-780)	1869 (1466-2144)	232 (120-398)	2114 (1867-2291)	3.6 (1.8-6.3)
Site 2	672 (234-1561)	2030 (1664-2264)	163 (68-314)	2214 (1984-2383)	2.5 (1.1-5.0)
Site 3	907 (262-5100)	2073 (1835-2365)	144 (25-243)	2246 (2089-2552)	2.2 (0.4-3.9)
Statistical significance	***	***	***	***	***

Temperature (T;  $n = 112$ -115 per site), pH ( $n = 103$ -110 per site) and salinity (S;  $n = 107$ -110 per site) were measured in July 2010, September 2010, November 2010, March 2011, June 2011, July-August 2011, November-December 2011, April-May 2012, June 2012 and May 2013. Total alkalinity (TA;  $n = 14$  per site) was measured in September 2010, November 2010, March 2011, June 2011, July-August 2011, November-December 2011, April-May 2012, June 2012 and May 2013.  $p\text{CO}_2$  = carbon dioxide partial pressure;  $\text{HCO}_3^-$  = bicarbonate;  $\text{CO}_3^{2-}$  = carbonate; DIC = dissolved inorganic carbon;  $\Omega_{\text{arag}}$  = aragonite saturation; NS = not significant; \*\*\* $p < 0.001$ , Kruskal-Wallis equality-of-populations rank test. In brackets the min and max values.

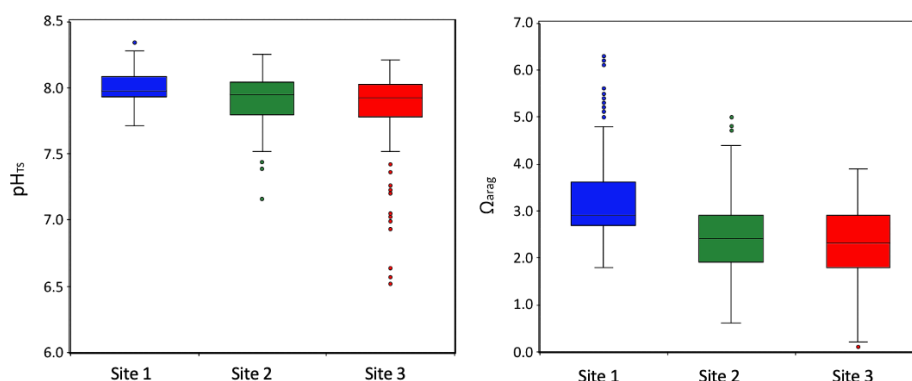


Figure 3. Ranges of measured  $\text{pH}_{\text{T}}$ s (number of observations [ $n$ ] = 185-198 per Site) and  $\Omega_{\text{arag}}$  ( $n = 184$ -195 per Site) values showing consistent decreases from Site 1 to Site 3. The boxes indicate the 25<sup>th</sup> and 75<sup>th</sup> percentiles and the line within the boxes mark the medians. Whisker length is equal to  $1.5 \times$  interquartile range (IQR). Circles represent outliers.

## Aim of the study

Assessing the effects of ocean acidification on reproduction of a model species: the Mediterranean coral *Balanophyllia europaea*.

## Background

Since the onset of industrialization, atmospheric concentrations of carbon dioxide (CO<sub>2</sub>) have increased at likely unparalleled rates. Approximately 40% of the CO<sub>2</sub> emitted into the atmosphere by human activities has been absorbed by the ocean (Feely et al. 2004; Gruber et al. 2019; Terhaar et al. 2022), causing significant changes to the carbonate chemistry (Feely et al. 2004). Surface ocean pH has decreased by 0.1 units in comparison to preindustrial values and the Intergovernmental Panel on Climate Change predicts a further decrease by 0.06-0.32 units by the end of the century, causing a further increase by more than 100% in hydrogen ions concentration in global oceans (Cubasch et al. 2014).

Documenting and projecting the response of marine ecosystems to changing ocean chemistry has been of increasing concern in the scientific community (Duarte 2014). Ocean acidification makes it difficult for marine calcifiers, like corals, to build their calcium carbonate structures (Kleypas and Yates 2009). Weakening these structures affects their ability to survive and reproduce. The recovery and persistence of a population, and of a species, requires that reproduction and recruitment keep pace with the loss of adult individuals (Santiago-Valentín et al. 2019). However, environmental factors can disrupt these processes, resulting in compromised recruitment or recruitment failure and profoundly affecting marine population dynamics (Gaines and Roughgarden 1985; Riegl et al. 2009).

Reproduction and early life history stages of different organisms are affected by acidification in terms of: larval availability (gamete production, fertilization etc.; (Kurihara et al. 2004; Reuter et al. 2011; Swiezak et al. 2018), larval development (Byrne 2011; Kurihara 2008; Lenz et al. 2019) and growth (Kurihara et al. 2004; Lenz et al. 2019), larval settlement (Kurihara 2008), post-settlement growth and survival (Byrne 2011). Nonetheless, limited information is available on the effects of ocean acidification on sexual reproduction in corals. Gametogenesis can extend over 9–11 months for some species (Babcock et al. 1986; Vargas-Angel et al. 2006), making studies on coral gamete development challenging when performed under controlled conditions, because maintaining colonies under experimental conditions for this period of time can be challenging. The aquaria and mesocosm experiments that have been conducted so far on the impact of ocean acidification on coral reproduction have shown negative effects on sperm motility (Morita et al. 2010; Nakamura and Morita 2012), fertilization process (Albright and Mason 2013) and early life stages, including larval development and settlement (Albright and Langdon 2011; Albright et al. 2010).

Carbon dioxide (CO<sub>2</sub>) vents, also known as natural carbon dioxide seeps, are areas in the ocean where CO<sub>2</sub> is naturally released from the seafloor (Aiuppa et al. 2021). These vents provide a unique opportunity to study the effects of ocean acidification on marine organisms in a natural setting, thus under conditions that cannot be mimicked in aquaria (e.g., currents, nutrients, prey-predator interactions (Meron et al. 2013; Strahl et al. 2015). The CO<sub>2</sub> vent off Panarea Island (Sicily, Italy) has been extensively studied in the past decade (Capaccioni et al. 2007; Caroselli et al. 2019; Fantazzini et al. 2015; Goffredo et al. 2014; Prada et al. 2017; Prada et al. 2023; Saidi et al. 2023; Sani et al. 2024) and represents an ideal natural laboratory for ocean acidification studies. This vent creates a natural pH gradient (ranging from pH<sub>TS</sub> 8.1 to 7.4) that allows investigating the effects of ocean acidification on marine life, including corals, across a range of pH levels, providing a glimpse into potential future scenarios driven by increased carbon dioxide emissions. At the most acidic site along this gradient, the solitary coral *Leptopsammia pruvoti*, transplanted for 3-4 months, experiences a slight postponement in sperm release, fertilization, and embryo formation (Gizzi et al. 2017). Likewise, spermary development and the fertilization process are delayed by decreasing pH in the colonial non-zooxanthellate coral *Astroides calycularis* exposed for 3 months under the same experimental conditions (Marchini et al. 2021). The present study investigated the short-term influence of decreasing seawater pH on the reproductive output of the solitary zooxanthellate coral *Balanophyllia europaea* transplanted along the same pCO<sub>2</sub> gradient. We hypothesize that the symbiotic relationship with photosynthetic algae, which utilize

CO<sub>2</sub> as a substrate for photosynthesis and energy production, might render zooxanthellate corals more resilient to ocean acidification than non-zooxanthellate corals. This resilience could result from enhanced productivity of Symbiodiniaceae photosynthesis under acidified conditions, enhancing energy production and providing an energetic advantage that helps mitigate the physiological stress of ocean acidification (Biscéré et al. 2019).

### ***A model species***

*Balanophyllia europaea* (Risso, 1826) is a solitary, zooxanthellate scleractinian coral, which lives on rocky substratum and is endemic to the Mediterranean Sea, where it is found at depths from 0 to 50. Its reproductive biology, growth, population dynamics and abundance, skeletal mechanical properties, and photosynthetic efficiency have been extensively studied throughout the Mediterranean and its conservation status assessed (Goffredo et al. 2004; Caroselli et al. 2020 and references therein; Otero et al. 2017). In particular, the studies conducted on natural populations of *B. europaea* living along the Panarea pH gradient (see video: [https://static-content.springer.com/esm/art%3A10.1038%2Fncmms8785/MediaObjects/41467\\_2015\\_BFncmms8785\\_MOESM429\\_ESM.mov](https://static-content.springer.com/esm/art%3A10.1038%2Fncmms8785/MediaObjects/41467_2015_BFncmms8785_MOESM429_ESM.mov) from Fantazzini et al. 2015) show that lower and variable pH conditions reduce calcification, skeletal density, and resistance, while linear extension is preserved (Fantazzini et al. 2015), allowing *B. europaea* to reach size at sexual maturity and reproduce (Caroselli et al. 2019) (Figure 4). The fraction of young individuals and recruitment efficiency strongly decrease at lower and variable pH<sub>TS</sub> (Caroselli et al. 2019), in agreement with the observed decrease in population abundance (Goffredo et al. 2014). A recent study shows that *B. europaea* physiologically adjusts to decreasing pH through changes in the density of zooxanthellae and their haplotypes, which ultimately affect the amount of photosynthetically fixed carbon relative to heterotrophically acquired carbon in the host (*under review*). Furthermore, the acquisition of symbiont strains potentially better adapted to acidified conditions could further contribute to increased nutrient cycling and animal growth (*under review*). Enhanced N<sub>2</sub> fixation by diazotrophs living in association with the coral tissue/mucus (Palladino et al. 2022) may partially explain the observed increase in dinoflagellate symbiont cell densities in *B. europaea* at the low pH Sites, and viceversa, enhanced translocation of photosynthetically fixed carbon as a result of high dinoflagellate symbiont cell densities may help sustain the high costs of diazotroph N<sub>2</sub> fixation under increased acidification. Additionally, as coral calcification and N<sub>2</sub> fixation by coral-associated diazotrophs are both energy-intensive processes, they probably compete for energy deriving from photosynthesis within the coral holobiont. Thus, the massive N<sub>2</sub> fixation occurring at the low pH Sites could be absorbing most of the photosynthetic energy from the symbiotic algae, creating an energy deficit that could possibly explain the previously observed decline in net calcification rates of this species along the same pH gradient (Fantazzini et al. 2015).

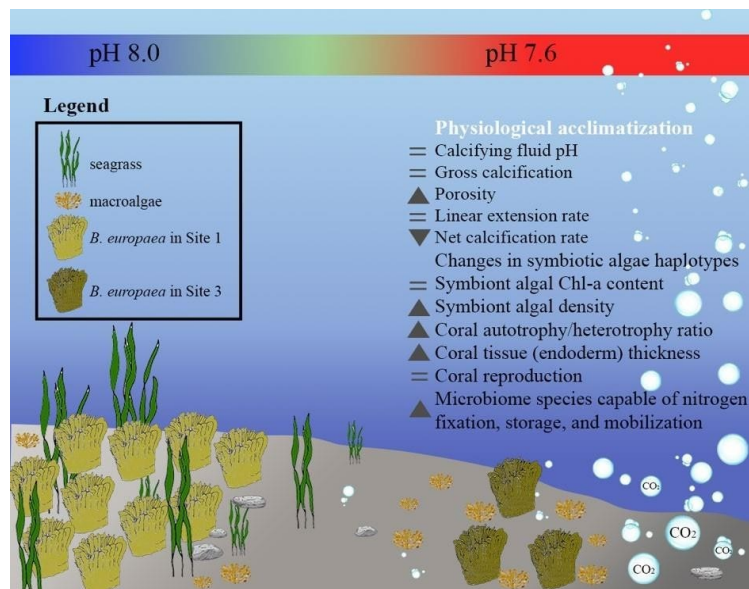


Figure 4. Conceptual scheme summarizing the effects of life-long physiological acclimatization to low pH/high  $p\text{CO}_2$  conditions in *B. europaea* at the Panarea  $\text{CO}_2$  vent. Under low pH conditions, coral population density decreases, net calcification is depressed, while linear extension rate is maintained constant, allowing the coral to reach critical size at sexual maturity and reproduce. Moreover, an overall rearrangement of the coral holobiont is documented by: i) an increase in zooxanthellae density, triggered by thickening of the coral tissue and the establishment of novel symbiont algal haplotypes possibly better adapted to lower pH conditions, and ii) an increase, within the coral tissue/mucus in microbial communities capable of  $\text{N}_2$  fixation as well as N storage and mobilization. Variations displayed by corals living at average pH 7.6 compared to corals at average pH 8.0 are shown with grey symbols and are listed in the following order: skeleton (from micro to macro), symbiotic algae (from micro to macro), trophic strategy, reproduction, tissue/mucus microbial community. Darker and lighter shades of green in the coral sketches represent higher and lower symbiont algal density. The color scale bar highlighting the seawater pH change across the gradient does not match the color scale of pH test strips. (*under review*)

## Methods

### Study site

The experimental field was located near Panarea Island (Mediterranean Sea, Italy,  $38^\circ 38' 16.98'' \text{ N}$ ;  $15^\circ 6' 37.26'' \text{ E}$ ) and is a part of an active volcanic system (De Astis et al. 2003). An underwater crater (20 x 14 m wide) characterized by continuous and localized emissions of almost pure  $\text{CO}_2$  (98-99% of  $\text{CO}_2$ ) at ambient temperature, lacking toxic compounds (e.g.  $\text{H}_2\text{S}$ ), generates a natural pH gradient (Prada et al. 2017; Prada et al. 2023). By investigating organisms along transects radiating from the sources of  $\text{CO}_2$ , we can assess how they respond to pH values along this gradient that match Intergovernmental Panel on Climate Change (IPCC) scenarios predicted for the end of the century. Along this gradient, four sites, whose seawater physicochemical parameters have been extensively characterized (Capaccioni et al. 2007; Goffredo et al. 2014; Prada et al. 2017; Prada et al. 2023), were selected: the control site (site 1, mean Total Scale (TS)  $\text{pH}_{\text{TS}}$  8.07) located  $\sim 34$  m away from the center of the crater, representing the current condition, two intermediate pH sites (site 2,  $\text{pH}_{\text{TS}}$  7.87 and site 3,  $\text{pH}_{\text{TS}}$  7.74), that align with IPCC's mean pH prediction of a conservative  $\text{CO}_2$  emissions scenario (Representative Concentration Pathway, RCP6.0), and a "business-as-usual"  $\text{CO}_2$  emissions scenario (RCP8.5), respectively, and an extreme pH site (site 4,  $\text{pH}_{\text{TS}}$  7.40) closer to the vents, representing the projection for 2300 (Figure 5) (Collins et al. 2014).

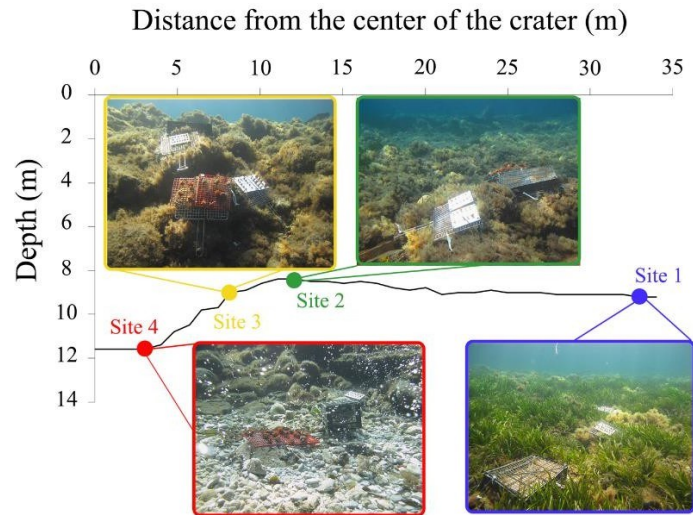


Figure 5. Bathymetric profile of the four sites. The pictures show representative images of the four sites and transplanted corals (under review).

### Sampling

Specimens of *Balanophyllia europaea* were collected by SCUBA diving at Pietra Nave, ~ 2 km away from the experimental field, where the species grows naturally at 3-6 m depth. Sampled corals were placed in a container with seawater and transported within 30 min by boat to the wet lab that was temporarily set up at the Eolo Sub Diving Center. Upon arrival at the diving center, *B. europaea* polyps were randomly assigned to each of the four Sites (n = 4 - 6 polyps per site, per experimental period) and glued with a non-toxic bicomponent epoxy coral glue (Milliput, Wales, UK) onto ceramic tiles (Figure 5). Corals were maintained at ambient temperature in containers aerated with a bubbler and no source of artificial light for 1d prior to transplantation. Corals were subjected to experimental conditions in different moments of their reproductive cycle (more details in section Definitions). The collected specimens were fixed in a formaldehyde fixative solution (90% seawater and 10% formaldehyde buffered with calcium carbonate) and transferred to the Department of Biological, Geological and Environmental Sciences (BiGeA) of the University of Bologna for histological analysis.

### Biometric measurements

Biometric analyses will be performed by measuring length (L, maximum axis of the oral disc), width (W, minimum axis of the oral disc) and height (H, distance between the oral and aboral disc) of each polyp using a caliper ( $\pm 0.05$  mm). These parameters allow to estimate the body volume (V) of the polyp using the following equation:  $V = H \cdot (L/2) \cdot (W/2) \cdot \pi$  (Goffredo et al. 2002). The volume will be used to calculate the reproductive parameters (see the Definitions section).

### Histological analysis

Polyps will be washed under running tap water for one night and post-fixed in Bouin solution for 24h. After decalcification with ethylenediaminetetraacetic acid and dehydration in increasing concentration of ethanol (from 70% to 100%), polyps will be clarified in histolemon and embedded in paraffin. Serial transverse sections will be cut at 7  $\mu$ m intervals along the oral-aboral axis, from the oral to the aboral pole of the polyp. Tissues will be then stained with Mayer's haematoxylin and eosin (Goffredo et al. 2002).

### Cyto-histometric analysis

Cyto-histometric analyses will be performed using an optical NIKON eclipse 80i microscope with the image analysis software NIKON NIS-Elements D 3.1 that allows to trace and measure the perimeter and area of the reproductive element. From these two parameters we will obtain the maximum and minimum diameters of all spermaries observed in the section every 7 slides and all oocytes observed in nucleate sections. Spermaries will

be also classified into five maturation stages distinguishable by morphological traits described in previous studies on coral gametogenesis (Fadlallah and Pearse 1982; Glynn et al. 2000; Goffredo et al. 2002). The presence of all embryos observed in the coelenteric cavity will be recorded and their maturation stage will be identified (Goffredo and Telò 1998). The size of each reproductive element and each embryo will be determined as the mean of the two diameters (Goffredo et al. 2002). The polyps without germ cells will be classified as sexually inactive individuals.

### Definitions

Reproductive output will be defined through six reproductive parameters: i) oocyte and spermary abundance, defined as the number of reproductive elements per body volume unit ( $100 \text{ mm}^3$ ); ii) gonadal index, defined as the percentage of the polyp body volume occupied by reproductive elements (the volume of each reproductive element will be measured as described in the subsection "Gonadal index" of (Goffredo et al. 2002)); iii) reproductive element diameter, defined as the average of the maximum and minimum diameter of spermaries and oocytes in nucleate sections; iv) fertility, defined as the number of embryos per body volume unit ( $100 \text{ mm}^3$ ) (Marchini et al. 2015); v) Embryonal index, defined as the percentage of the polyp body volume occupied by embryos; vi) embryo diameter, defined as the average of the maximum and minimum diameter of embryos. Based on the reproductive season, the reproductive cycle of *B. europaea* will be divided in two gamete activity periods: i) gonadal development period, characterized by the presence of small immature oocyte ( $< 400 \mu\text{m}$ ), spermaries in the early stages of development, and embryos in the coelenteric cavity of female polyps. This period includes polyps from the following two sampling campaigns: transplant at the beginning of June 2011 and collection at the end of July 2011, and transplant at the end of April 2012 and collection at the end of June 2012; ii) maturity period, characterized by the presence of two distinct oocyte stocks, one made of smaller immature cell ( $< 400 \mu\text{m}$ ) and the other made of big mature cell ( $> 400 \mu\text{m}$ ). Spermaries will be present at all the development stages in the same sample (I, II, III, IV, V). This period includes polyps from the following two sampling campaigns: transplant in mid-December 2010 and collection in March 2011, and transplant at the beginning of December and collection in April 2012.

### REFERENCES

- Aiuppa, A., J. M. Hall-Spencer, M. Milazzo, G. Turco, S. Caliro, and R. Di Napoli. 2021. Volcanic CO<sub>2</sub> seep geochemistry and use in understanding ocean acidification. *Biogeochemistry* **152**: 93-115.
- Albright, R., and C. Langdon. 2011. Ocean acidification impacts multiple early life history processes of the Caribbean coral. *Global Change Biol* **17**: 2478-2487.
- Albright, R., and B. Mason. 2013. Projected near-future levels of temperature and pCO<sub>2</sub> reduce coral fertilization success. *Plos One* **8**: e56468.
- Albright, R., B. Mason, M. Miller, and C. Langdon. 2010. Ocean acidification compromises recruitment success of the threatened Caribbean coral. *P Natl Acad Sci USA* **107**: 20400-20404.
- Babcock, R. C. and others 1986. Synchronous spawnings of 105 scleractinian coral species on the Great Barrier Reef. *Mar Biol* **90**: 379-394.
- Biscéré, T. and others 2019. High pCO<sub>2</sub> promotes coral primary production. *Biol Letters* **15**: 20180777.
- Byrne, M. 2011. Impact of ocean warming and ocean acidification on marine invertebrate life history stages: vulnerabilities and potential for persistence in a changing ocean. *Oceanogr Mar Biol* **49**: 1-42.
- Capaccioni, B., F. Tassi, O. Vaselli, D. Tedesco, and R. Poreda. 2007. Submarine gas burst at Panarea Island

(southern Italy) on 3 November 2002: A magmatic versus hydrothermal episode. *Journal of Geophysical Research* **112**: B05201.

Caroselli, E. and others 2019. Low and variable pH decreases recruitment efficiency in populations of a temperate coral naturally present at a CO<sub>2</sub> vent. *Limnol Oceanogr* **64**: 1059-1069.

Caroselli, E., H. B. Ozalp, M. Lavia, F. De Witt, F. Raimondi, S. Goffredo. 2020. Population dynamics of a temperate coral along a depth gradient in the Dardanelles. *Limnology & Oceanography* **65**:2676- 2687.

Collins, M. and others 2014. Long-term Climate Change: Projections, Commitments and Irreversibility. *Climate Change 2013: The Physical Science Basis*: 1029-1136.

Cubasch, U. and others 2014. Climate Change 2013 The Physical Science Basis Working Group I Contribution to the Fifth Assessment Report of the Intergovernmental Panel on Climate Change Introduction. *Climate Change 2013: The Physical Science Basis*: 119-158.

De Astis, G., G. Ventura, G. Vilardo. 2003. Geodynamic significance of the Aeolian volcanism (Southern Tyrrhenian Sea, Italy) in light of structural, seismological, and geochemical data. *Tectonics* **22**:1040.

Duarte, C. M. 2014. Global change and the future ocean: a grand challenge for marine sciences. *Front Mar Sci* **1**.

Fadlallah, Y. H., and J. S. Pearse. 1982. Sexual reproduction in solitary corals - overlapping oogenic and brooding cycles, and benthic planulas in *Balanophyllia elegans*. *Mar Biol* **71**: 223-231.

Fantazzini, P. and others 2015. Gains and losses of coral skeletal porosity changes with ocean acidification acclimation. *Nat Commun* **6**: 7785.

Feely, R. A. and others 2004. Impact of Anthropogenic CO<sub>2</sub> on the CaCO<sub>3</sub> System in the Oceans. *Science* **305**: 362-366.

Gaines, S., and J. Roughgarden. 1985. Larval Settlement Rate - a Leading Determinant of Structure in an Ecological Community of the Marine Intertidal Zone. *P Natl Acad Sci USA* **82**: 3707-3711.

Gizzi, F. and others 2017. Reproduction of an azooxanthellate coral is unaffected by ocean acidification. *Sci Rep-Uk* **7**: 1-8.

Glynn, P. W., S. B. Colley, J. H. Ting, J. L. Maté, and H. M. Guzmán. 2000. Reef coral reproduction in the eastern Pacific: Costa Rica, Panama and Galapagos Islands (Ecuador). IV. Agariciidae, recruitment and recovery of *Pavona varians* and *Pavona* sp.a. *Mar Biol* **136**: 785-805.

Goffredo, S., and T. Telò. 1998. Hermaphroditism and brooding in the solitary coral *Balanophyllia europaea* (Cnidaria, Anthozoa, Scleractinia). *Ital J Zool* **65**: 159-165.

Goffredo, S., S. Arnone, and F. Zaccanti. 2002. Sexual reproduction in the Mediterranean solitary coral (Scleractinia, Dendrophylliidae). *Mar Ecol Prog Ser* **229**: 83-94.

Goffredo, S., G. Mattioli, F. Zaccanti. 2004: Growth and population dynamics model of the Mediterranean solitary coral *Balanophyllia europaea* (Scleractinia, Dendrophylliidae). *Coral Reefs* **23**: 433-443.



Goffredo, S. and others 2014. Biomineralization control related to population density under ocean acidification. *Nat Clim Change* **4**: 593-597.

Gruber, N. and others 2019. The oceanic sink for anthropogenic CO<sub>2</sub> from 1994 to 2007. *Science* **363**: 1193-1199.

Kleypas, J. A., and K. K. Yates. 2009. Coral reefs and ocean acidification. *Oceanography* **22**: 108-117.

Kurihara, H. 2008. Effects of CO<sub>2</sub>-driven ocean acidification on the early developmental stages of invertebrates. *Mar Ecol Prog Ser* **373**: 275-284.

Kurihara, H., S. Shimode, and Y. Shirayama. 2004. Effects of raised CO<sub>2</sub> concentration on the egg production rate and early development of two marine copepods (*Acartia steueri* and *Acartia erythraea*). *Mar Pollut Bull* **49**: 721-727.

Lenz, B., N. D. Fogarty, and J. Figueiredo. 2019. Effects of ocean warming and acidification on fertilization success and early larval development in the green sea urchin. *Mar Pollut Bull* **141**: 70-78.

Marchini, C. and others 2015. Annual reproductive cycle and unusual embryogenesis of a temperate coral in the Mediterranean Sea. *Plos One* **10**: e0141162.

Marchini, C. and others 2021. Decreasing pH impairs sexual reproduction in a Mediterranean coral transplanted at a CO<sub>2</sub> vent. *Limnol Oceanogr* **66**: 3990-4000.

Meron, D., M. C. Buia, M. Fine, and E. Banin. 2013. Changes in microbial communities associated with the sea anemone *Anemonia viridis* in a natural pH gradient. *Microb Ecol* **65**: 269-276.

Morita, M. and others 2010. Ocean acidification reduces sperm flagellar motility in broadcast spawning reef invertebrates. *Zygote* **18**: 103-107.

Nakamura, M., and M. Morita. 2012. Sperm motility of the scleractinian coral *Acropora digitifera* under preindustrial, current, and predicted ocean acidification regimes. *Aquat Biol* **15**: 299-302.

Palladino, G., E. Caroselli, T. Tavella, F. D'Amico, F. Prada, A. Mancuso, S. Franzellitti, S. Rampelli, M. Candela, S. Goffredo, E. Biagi. 2022. Metagenomic shifts in mucus, tissue and skeleton of the coral *Balanophyllia europaea* living along a natural CO<sub>2</sub> gradient. *ISME Communications* **2**:65.

Prada, F. and others 2017. Ocean warming and acidification synergistically increase coral mortality. *Sci Rep-Uk* **7**.

Prada, F. and others 2023. Acclimatization of a coral-dinoflagellate mutualism at a CO<sub>2</sub> vent. *Communications Biology* **6**: 66.

Reuter, K. E., K. E. Lotterhos, R. N. Crim, C. A. Thompson, and C. D. G. Harley. 2011. Elevated pCO<sub>2</sub> increases sperm limitation and risk of polyspermy in the red sea urchin *Strongylocentrotus franciscanus*. *Global Change Biol* **17**: 2512-2512.

Riegl, B., S. J. Purkis, J. Keck, and G. P. Rowlands. 2009. Monitored and modeled coral population dynamics and the refuge concept. *Mar Pollut Bull* **58**: 24-38.

Saidi, A. and others 2023. Microbial dynamics in shallow CO<sub>2</sub> seeps system off Panarea Island (Italy). *Mar Biol* **170**: 1-4.

Sani, T. and others 2024. Ocean warming and acidification detrimentally affect coral tissue regeneration at a Mediterranean CO<sub>2</sub> vent. *Sci Total Environ* **906**: 167789.

Santiago-Valentín, J. D., A. P. Rodríguez-Troncoso, E. Bautista-Guerrero, A. López-Pérez, and A. L. Cupul-Magaña. 2019. Successful sexual reproduction of the scleractinian coral: Evidence of planktonic larvae and recruitment. *Invertebr Biol* **138**: 29-39.

Strahl, J., I. Stolz, S. Uthicke, N. Vogel, S. H. C. Noonan, and K. E. Fabricius. 2015. Physiological and ecological performance differs in four coral taxa at a volcanic carbon dioxide seep. *Comparative Biochemistry and Physiology a-Molecular & Integrative Physiology* **184**: 179-186.

Swiezak, J., A. R. Borrero-Santiago, A. Sokolowski, and A. J. Olsen. 2018. Impact of environmental hypercapnia on fertilization success rate and the early embryonic development of the clam *Limecola balthica* (Bivalvia, Tellinidae) from the southern Baltic Sea—A potential CO<sub>2</sub> leakage case study. *Mar Pollut Bull* **136**: 201-211.

Terhaar, J., T. L. Frölicher, and F. Joos. 2022. Observation-constrained estimates of the global ocean carbon sink from Earth system models. *Biogeosciences* **19**: 4431-4457.

Vargas-Angel, B., S. B. Colley, S. M. Hoke, and J. D. Thomas. 2006. The reproductive seasonality and gametogenic cycle of *Acropora cervicornis* off Broward County, Florida, USA. *Coral Reefs* **25**: 110-122.